Optics Communications 392 (2017) 208–213

Contents lists available at ScienceDirect

Optics Communications

journal homepage: www.elsevier.com/locate/optcom

All-optical XOR and NAND logic gates based on plasmonic nanoparticles

Najmeh Nozhat*, Hamid Alikomak, Maryam Khodadadi

Faculty of Electrical Engineering, Shiraz University of Technology, Shiraz, Iran

ARTICLE INFO

Keywords:
Logic gates
Plasmonic nanoparticles
High contrast ratio

ABSTRACT

In this paper, all-optical XOR and NAND logic gates based on gold disk-shaped nanoparticles have been proposed. The proposed structure consists of a non-periodic array of disk-shaped nanoparticles that are placed on SiO_2 substrate. The gates function is based on the constructive and destructive interferences between the input signals. For the NAND gate the phase difference between the input signals has been used to create a destructive interference. The most advantages of these structures are subwavelength dimensions and high contrast ratio of about 26 dB and 24 dB for the XOR and NAND logic gates, respectively.

1. Introduction

All-optical devices based on nanoparticles and effect of surface plasmons (SPs) play a great roll in integrated optical circuits due to nanoscale size, ultrahigh speed information processing, high capacity, low power consumption, security to electromagnetic interference and also overcoming the diffraction limit of light by surface plasmon polaritons (SPPs) [1–5]. Semiconductor devices suffer from heat generation and low speed so it was motivating to research more in field of optical computing. Recently, researches have proposed all-optical devices such as waveguides [6,7], junctions [8], sensors [9–12], switches [13,14], modulators [15,16] and logic gates [17] based on SPPs. Surface plasmons are observed in noble metals such as silver and gold in visible and near-infrared regions. Plasmonic nanoparticles are good candidates for utilizing in optical devices due to their absorption, scattering and coupling features that depend on the basic parameters such as geometry, dimension, and position of nanoparticles [18–22]. Also, researchers have proposed all-optical logic gates in hybrid plasmonic-photonic crystal nano-beam cavities [23] and nonophotonic plasmonics [17], according to waveguide type Kretchmann-Reather configuration on the metal surface [24], cross phase modulation (XPM) [25] and amplifier [26]. Moreover, all-optical logic gates based on linear interference between (SPP) modes in a silver nanowire network have been studied [17,27].

In this paper, a new XOR and NAND logic gates based on a non-periodic nano-disk array of gold nanoparticles placed on SiO_2 substrate have been proposed. The structures have been analyzed numerically by the finite-difference time-domain (FDTD) and analytically. The effect of nanoparticle distance on the localized surface plasmon resonances (LSPRs) has been studied. Highly reduction of size and loss are provided by proposed all-optical logic gates. We have obtained high contrast ratio of 26 dB and 24 dB for the XOR and NAND logic gates, respectively. The transmission of more than 90% is obtained for our structures. It is possible to utilize nanolithography techniques to implement the design of optical logic gates with accuracy of 5 nm for photonics integrated circuits (PICs) [28].

This paper is organized as follows. In Section 2, simulation method and theory concept have been presented. In Section 3, all-optical logic gates have been proposed, analyzed and compared with the previous works. The paper is concluded in Section 4.

2. Simulation method and theory concept

Our proposed structure, as shown in Fig. 1, consists of a 5 × 5 array of gold disk-shaped nanoparticles with the radius of a=50 nm, the height of h=20 nm and the inter-particle spacing of d=5 nm that are placed on SiO_2 substrate with the refractive index of 1.5. In our simulations Johnson and Christy data [29] is utilized to describe the gold permittivity, because Drude model is not able to model noble metals such as gold in our simulations frequency range.

The simulations are based on the finite-difference time-domain (FDTD) numerical method with the convolutional perfectly matched layer (CPML) as absorbing boundary condition. The structure is excited by a TM polarized pulse with electromagnetic filed components of H_z, E_x and E_y. Also, in our proposed structures, the output port C is along x or y axes for the XOR and NAND logic gates, respectively.

The transmission spectra of the structure of Fig. 1 for the inter-particle spacing of 0, 5, and 10 nm are illustrated in Fig. 2. The transmission spectrum has the maximum amplitude when the inter-particle spacing is 5 nm. Depending on the position and number of the

* Corresponding author.
E-mail address: nozhat@sutech.ac.ir (N. Nozhat).

http://dx.doi.org/10.1016/j.optcom.2017.02.007
Received 29 August 2016; Received in revised form 1 February 2017; Accepted 3 February 2017

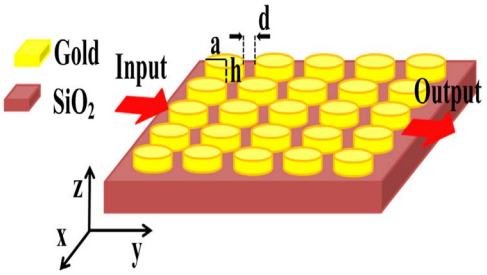

Fig. 1. Schematic view of a 5×5 array of gold disk-shaped nanoparticles placed on SiO_2 substrate.

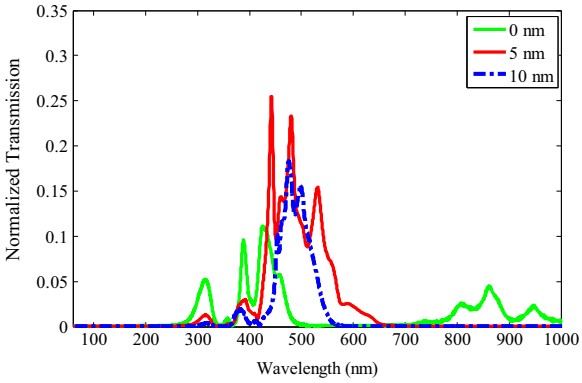

Fig. 2. Transmission spectra of the array structure of Fig. 1 with the inter-particle spacing of 0, 5, and 10 nm.

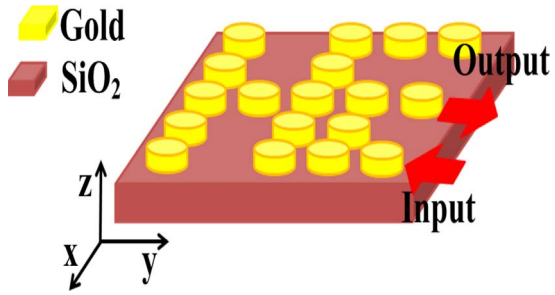

(a)

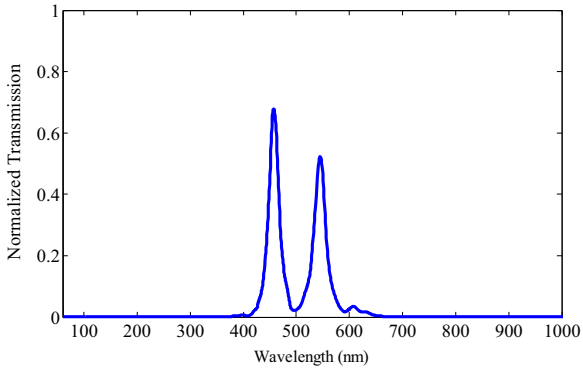

(b)

Fig. 3. (a) Schematic view of a non-periodic array of gold disk-shaped nanoparticles and (b) its transmission spectrum.

plasmonic nano-disks, the local field of each nanoparticle is minimized or maximized. The interaction between nano-disks in Fig. 1 causes new LSPRs which are a result of the coupling between the various individual LSPRs of the isolated particles. Furthermore, since plasmon waves couple strongly only in the near-field regime at very short distances, closely packed clusters is also needed to achieve high field enhancement. So if inter-particle spacing increases, the inter-field interferences decrease and the transmission spectrum of the array is similar to the typical nano-disk [30]. According to the obtained results, the optimum inter-particle spacing for the proposed structure has been chosen to be 5 nm.

In addition to the shape, size and material of nanoparticles, the properties of transmitted light strongly depend on the localized positions and gaps between nanoparticles. Plasmonic nanoparticles with periodic structures have been reported [31].

The optical absorption of a nanoparticle array can be directly obtained as follow [14]:

$$Q_{abs} = \frac{4\pi k}{|\mathbf{E}_0^2|\pi a^2} \sum_{i=1}^{N} \{\mathrm{Im}[\mathbf{P}_i(\alpha_i^{-1})^* \mathbf{P}_i^* - \frac{2}{3}k^3|\mathbf{P}_i|^2]\} \quad (1)$$

where k in the wave number, $\mathbf{E_0}$ and $\mathbf{P_i}$ are the incident electric field and the induced dipole moment, respectively. The polarizability (α_i) of each nanoparticle can be expressed as [14]:

$$\alpha_i = V\varepsilon_0 \frac{\varepsilon_r - 1}{1 + L(\varepsilon_r - 1)} \quad (2)$$

where $\varepsilon_r = \varepsilon_{particle}/\varepsilon_{medium}$, V is the particle volume and L is the shape factor that depends on the nanoparticle structure [31]:

On one hand, optical absorption is known as destructive phenomena and has to be suppressed but on the other hand, absorption control can be considered as a helpful feature in plasmonic waveguides. For instance, in order to obtain full coupling of the nano-disks, absorption of the nano-disks has to be controlled. Manipulation of nanoparticles can reveal the importance of absorption control. According to Eqs. (1) and (2), absorption depends on particle geometry, polarization and permittivity of the material. By decreasing the transmission, the absorption is increased.

One of the most promising plasmonics nanoparticle platforms is studying the effect of deterministic aperiodic structure of nanoparticles on the properties of transmitted light [16,31,32]. In this paper, it is intended to obtain a high transmission when one signal is applied to the proposed structure. As shown in Fig. 2, when the array is periodic, the transmission is low. The field of each nanoparticle is the result of the input source as well as other nanoparticles interaction [18]. Since the arrangement of nanoparticles significantly influences the fields of the structure, the nanoparticles must be rearranged non-periodically in a way that near-fields and far-fields strengthen each other [32].

The schematic view and the transmission spectrum of a non-periodic structure are shown in Fig. 3. By comparing Figs. 2 and 3b, it is clear that removing some nanoparticles and rearranging them in a non-periodic form have a great effect on the oscillation of nanoparticles and the transmission is much higher compared to the periodic one.

3. The proposed all-optical logic gates

3.1. XOR logic gate based on the non-periodic plasmonic nanoparticles

Exclusive OR (XOR) plays a significant role in logic optical circuits that the circuit symbol and truth table corresponding to its input-output are shown in Fig. 4 [33]:

The schematic view of the proposed XOR logic gate is shown in Fig. 5. A and B are the input ports and the output port is C. The parameters of the structure are chosen to be a=50 nm, h=20 nm, and d=5 nm. The nanoparticles are made of gold and the substrate is SiO_2.

The structure is illuminated by a narrow band plane wave with the central wavelength of 453 nm. According to the transmission spectrum of Fig. 6 surface plasmons are excited at the wavelength of 451.8 nm.

In the proposed XOR logic gate, A and B input ports are excited

(a)

A	B	A XOR B
0	0	0
0	1	1
1	0	1
1	1	0

(b)

Fig. 4. (a) The circuit symbol and (b) the truth table of XOR logic gate.

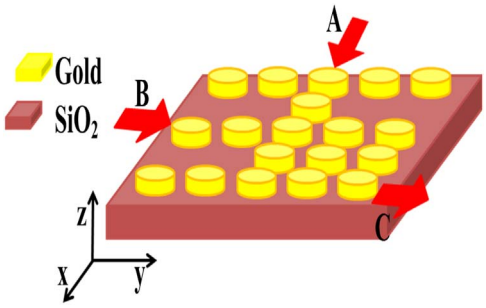

Fig. 5. Schematic view of the proposed XOR logic gate.

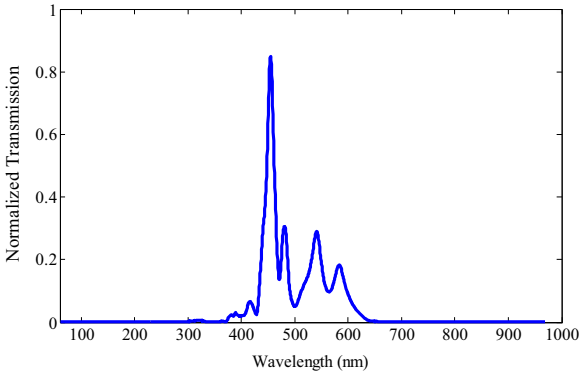

Fig. 6. Transmission spectrum of the structure of Fig. 5.

along x and y axes, respectively, and also, output port C is along y axis. The following equations describe the magnetic fields of two different inputs [33]:

$$\mathbf{H}^{Ai} = \vec{a}_z a_n^{Ai} \exp(jk_m x) = \vec{a}_z \sum_{n=-\infty}^{\infty} a_n^{Ai} j^n J_n(k_m \rho) \exp(jn\varphi), \tag{3}$$

$$\mathbf{H}^{Bi} = \vec{a}_z a_n^{Bi} \exp(jk_m y) = \vec{a}_z \sum_{n=-\infty}^{\infty} a_n^{Bi} j^n J_n(k_m \rho) \exp\left(jn\left(\varphi - \frac{\pi}{2}\right)\right), \tag{4}$$

where a_n^{Ai} and a_n^{Bi} are the amplitudes of two magnetic field sources. Radial distance and azimuth angel are ρ and φ, respectively. Thus, the transmitted magnetic fields to nanoparticles will be:

$$\mathbf{H}^{At} = \vec{a}_z \sum_{n=-\infty}^{\infty} a_n^{At} j^n J_n(k_d \rho) \exp(jn\varphi) \tag{5}$$

$$\mathbf{H}^{Bt} = \vec{a}_z \sum_{n=-\infty}^{\infty} a_n^{Bt} j^n J_n(k_d \rho) \exp\left(jn\left(\varphi - \frac{\pi}{2}\right)\right) \tag{6}$$

When n=2 and $a_n^{Ai} = a_n^{Bi} \neq 0$ (i.e, both inputs are in high logic level) the total magnetic field using Eqs. (5) and (6) can be calculated as [33]:

$$\mathbf{H}^{t}_{n=2}(\rho \leq a, \varphi) = \mathbf{H}^{At}_{n=2} + \mathbf{H}^{Bt}_{n=2} = 0 \tag{7}$$

It can be understood from Eq. (7) that the inputs (A and B) are assumed to be simultaneously equal at high level value; so the output logic in this case will be zero, because the second resonance mode cannot be generated. Thus, without this assumption the output will be in high logic level. In order to minimize the loss of the logic gate, the two input sources must be located in the same distance to nanoparticle.

The following example describes the qualitative performance of our proposed structure. Consider A and B are in high logic level. In this case, there are two ports to excite LSPRs as A and B inputs of the logic gate. As two sources are symmetric and also out of phase, the waves decreased each other and make a null mode in the output that causes low logic level.

By launching a continuous wave (CW) at the wavelength of 451.8 nm to the input port A or B, the value of transmission at port C is 0.95 which gives logic1. When two input ports are simultaneously excited by a lightwave with the resonance wavelength of 451.8 nm, the destructive interference occurs between two input signals and so the value of the transmission at the output port C is 0.09 that would be logic 0. The transmission spectra and magnetic field (H_z) distributions of the proposed XOR logic gate are demonstrated in Figs. 7–9.

The contrast ratio between the ON and OFF states is defined as [33]:

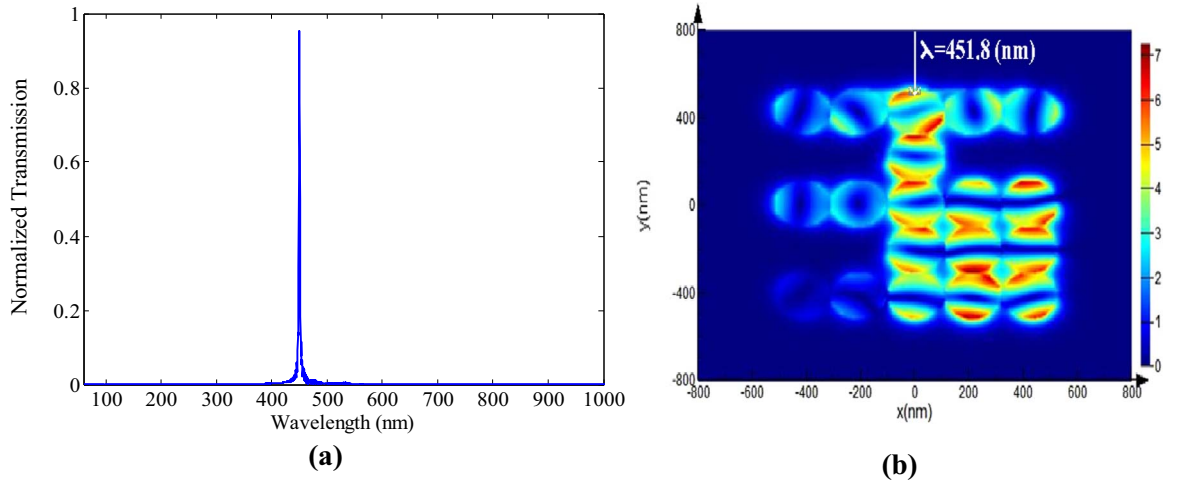

Fig. 7. (a) Transmission spectrum and (b) magnetic field (H_z) distribution of the proposed XOR logic gate when a CW wave is launched to the input port A (A=1, B=0).

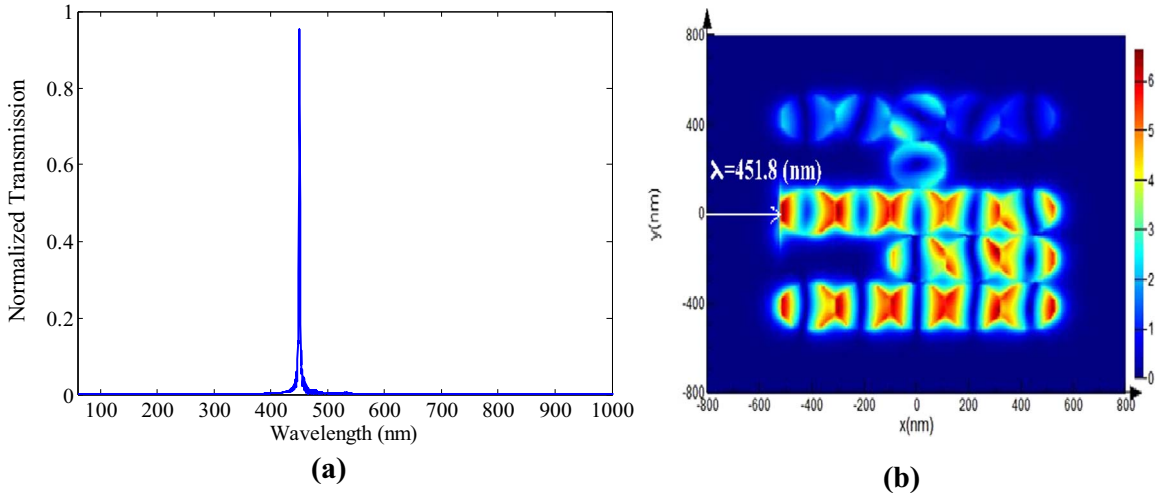

Fig. 8. (a) Transmission spectrum and (b) magnetic field (H_z) distribution of the proposed XOR logic gate when a CW wave is launched to the input port B (A=0, B=1).

$$\frac{\text{ON}}{\text{OFF}} = 10log\left(\frac{P_{out/ON}}{P_{out/OFF}}\right) \quad (8)$$

The contrast ratio of the proposed XOR logic gate, according to Eq. (8), is obtained to be 26 dB.

3.2. NAND logic gate based on the non-periodic plasmonic nanoparticles

NAND is a logic circuit element that its circuit symbol and the truth table are shown in Fig. 10 [33]:

The proposed structure of the NAND gate is based on Fig. 11. The structural parameters of this logic gate are the same as XOR gate. By launching a plane wave to the input port A, the resonance wavelength of the nanoparticles is obtained to be 445.5 nm.

In the proposed NAND gate, the relative location of the input and control sources can be adjusted to provide the desired intensity at the nanoparticle. Three similar sources are supposed to be at different locations in the proposed NAND structure. To realize low logic state, two input waves must be diminished by the wave from the control source [33]:

$$\mathbf{H}^{Ai}|_{X=X_1} + \mathbf{H}^{Bi}|_{X=X_1} = \mathbf{H}^{control}|_{X=X_1} \quad (9)$$

The phase difference between the input ports is used to create a destructive interference. When there is no lightwave at the input ports A and B, the control signal with the resonant wavelength of 445.5 nm is

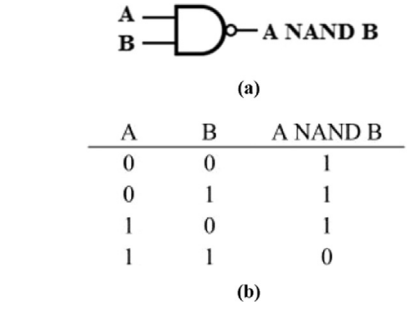

A	B	A NAND B
0	0	1
0	1	1
1	0	1
1	1	0

(b)

Fig. 10. (a) The circuit symbol and (b) the truth table of NAND logic gate.

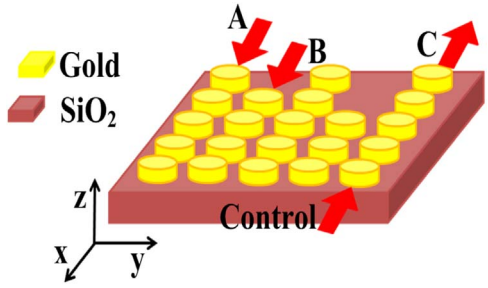

Fig. 11. Schematic view of the proposed NAND logic gate.

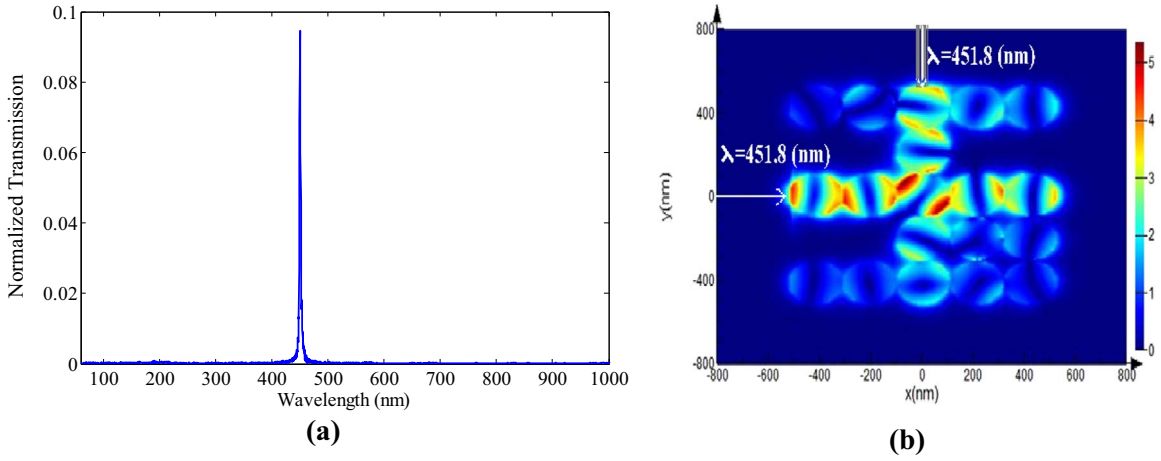

Fig. 9. (a) Transmission spectrum and (b) magnetic field (H_z) distribution of the proposed XOR logic gate when a CW wave is launched to the input ports A and B simultaneously (A=1, B=1).

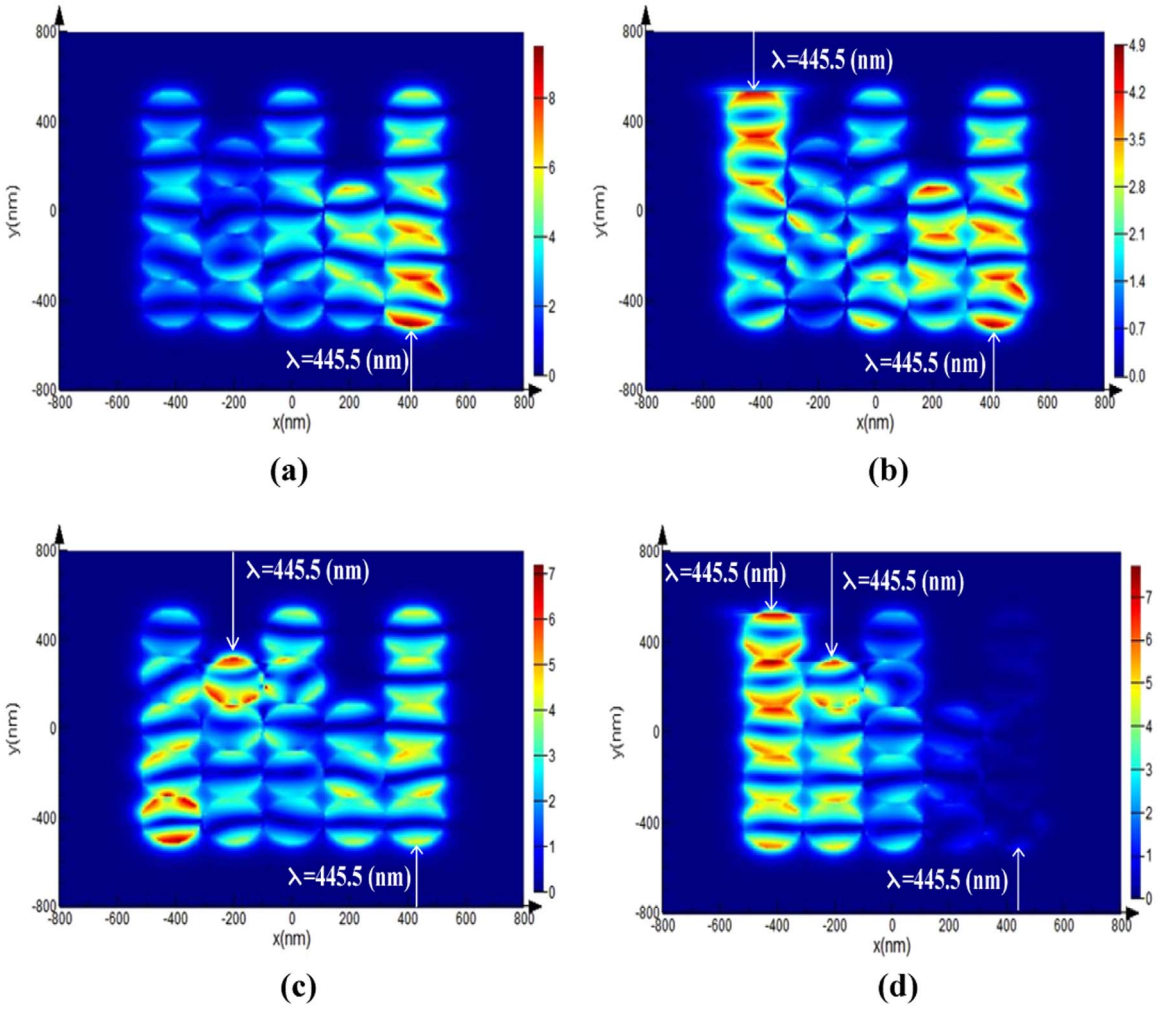

Fig. 12. Magnetic field (H_z) distributions of the proposed NAND gate when (a) there is no signal at the input ports A and B, a CW wave is launched to the (b) input port A, (c) input port B, and (d) input ports A and B, simultaneously. In all states, a control signal is applied at control port.

Table 1
Comparison between our proposed structures and previous works.

Criteria	This paper	Ref [33]	Ref [34]	Ref [35]	Ref [36]
Structure	Plasmonic nano-particle	Plasmonic Waveguide nano-disk	Plasmonic Waveguide	Plasmonic Waveguide	Plasmonic Waveguide
Noble metal	Gold	Silver	Silver	Silver	Silver
Proposed device	XOR and NAND logic gates	NOT, XOR, XNOR, and NAND logic gates	Switch	Switch	AND, OR, and NOT logic gates
Size	Smaller than 60 nm	Larger than 500 nm	Micrometer	Micrometer	Micrometer
Order of the wavelength operation	Nanometer	Nanometer	Micrometer	Micrometer	Micrometer
Loss	Low	Not very low	High	High	High

passed through the structure and the output transmission is 0.91 which gives logic 1. When one of the input ports is excited by a continuous wave (CW) with the wavelength of 445.5 nm, the transmission at the output port C is 0.92 and port C is ON. However, when two input ports A and B are excited simultaneously, the transmission of the output port C becomes 0.03 which would be logic 0. The magnetic field (H_z) distributions of the NAND gate are shown in Fig. 12. The contrast ratio between the ON and OFF states is 24 dB.

3.3. The comparison of the current paper and the previous papers

The proposed logic gates are compared to the previous structures as depicted in Table 1. In addition to the information of the Table 1, in our proposed structure not only one substrate is needed but also the transmission is more than 90%.

The field caused by nanoparticle is generated by input laser and other nanoparticle field interactions. Nanoparticle polarization depends on the direction of the input laser. Also, the generated fields are destructive or constructive according to the nanoparticle layout.

4. Conclusion

In this paper, effects of nanoparticle distance and periodicity of gold disk-shaped nanoparticles on the localized surface plasmon resonances (LSPRs) have been studied. Then, XOR and NAND logic gates based on a non-periodic array of gold disk-shaped nanoparticles that are placed

on SiO_2 substrate have been proposed and investigated. The operational principles of these gates are based on the constructive and destructive interferences caused by the difference in path length and the direction of the input signals. The high contrast ratio of about 26 dB and 24 dB has been attained for the XOR and NAND logic gates, respectively.

References

[1] W.L. Barnes, A. Dereux, T.W. Ebbesen, Surface plasmon subwavelength optics, Nature 424 (2003) 824–830.
[2] Q. Zhang, X.G. Huang, X.S. Lin, J. Tao, X.P. Jin, A subwavelength coupler-type MIM optical filter, Opt. Express 17 (2009) 7549–7555.
[3] N. Talebi, A. Mahjoubfar, M. Shahabadi, Plasmonic ring resonator, J. Opt. Soc. Am. B 25 (2008) 2116–2122.
[4] D.K. Gramotnev, S.I. Bozhevolnyi, Plasmonics beyond the diffraction limit, Nat. Photonics 4 (2010) 83–91.
[5] E. Ozbay, Plasmonics: merging photonics and electronics at nanoscale dimensions, Science 311 (2006) 189–193.
[6] J.H. Jung, Optimal design of dielectric-loaded surface plasmon polariton waveguide with genetic algorithm, J. Opt. Soc. Korea 14 (2010) 277–281.
[7] B. Jafarian, N. Nozhat, N. Granpayeh, Analysis of a triangular-shaped plasmonic metal-insulator-metal Bragg grating waveguide, J. Opt. Soc. Korea 15 (2011) 118–123.
[8] M. Farahani, N. Granpayeh, M. Rezvani, Broadband zero reflection plasmonic junctions, J. Opt. Soc. Am. B 29 (2012) 1722–1730.
[9] J.H. Jung, M.W. Kim, Optimal design of fiber-optic surface plasmon resonance sensors, J. Opt. Soc. Korea 11 (2007) 55–58.
[10] K.M. Byun, Development of nanostructured plasmonic substrates for enhanced optical biosensing, J. Opt. Soc. Korea 14 (2010) 65–76.
[11] J. Becker, A. Trügler, A. Jakab, U. Hohenester, C. Sönnichsen, The optimal aspect ratio of gold nanorods for plasmonic bio-sensing, Plasmonics 5 (2010) 161–167.
[12] J. Katyal, R. Soni, Localized surface plasmon resonance and refractive index sensitivity of metal–dielectric–metal multilayered nanostructures, Plasmonics 9 (2014) 1171–1181.
[13] H. Lu, X. Liu, L. Wang, Y. Gong, D. Mao, Ultrafast all-optical switching in nanoplasmonic waveguide with Kerr nonlinear resonator, Opt. Express 19 (2011) 2910–2915.
[14] M. Akhlaghi, N. Nozhat, F. Emami, Investigating the optical switch using dimer plasmonic nano-rods, IEEE Trans. Nanotechnol. 13 (2014) 1172–1175.
[15] F. Emami, M. Akhlaghi, N. Nozhat, Binary optimization of gold nano-rods for designing an optical modulator, J. Comput. Electron. 14 (2015) 574–581.
[16] M. Akhlaghi, N. Nozhat, F. Emami, High speed optical FSK demodulator using plasmonic nano rods, J. Mod. Opt. 62 (2015) 307–312.
[17] H. Wei, Z. Wang, X. Tian, M. Käll, H. Xu, Cascaded logic gates in nanophotonic plasmon networks, Nat. Commun. 2 (2011) 387–391.
[18] S.A. Maier, Plasmonics: Fundamentals and Applications, Springer, USA, 2007.
[19] K. Liou, Y. Takano, P. Yang, Light absorption and scattering by aggregates: application to black carbon and snow grains, J. Quant. Spectrosc. Radiat. Transf. 112 (2011) 1581–1594.
[20] E. Ringe, J. Zhang, M.R. Langille, K. Sohn, C. Cobley, L. Au, et al., Effect of size, shape, composition, and support film on localized surface plasmon resonance frequency: a single particle approach applied to silver bipyramids and gold and silver nanocubes (MA, United States)Mater. Res. Soc. Symp. Proc. Boston (2009) 52–57.
[21] S.Q. Li, P. Guo, L. Zhang, W. Zhou, T.W. Odom, T. Seideman, J.B. Ketterson, R.P.H. Chang, Infrared plasmonics with indium–tin-oxide nanorod arrays, ACS Nano 5 (2011) 9161–9170.
[22] M. Hu, C. Novo, A. Funston, H. Wang, H. Staleva, S. Zou, P. Mulvaney, T. Xia, G.V. Hartland, Dark-field microscopy studies of single metal nanoparticles: understanding the factors that influence the linewidth of the localized surface plasmon resonance, J. Mater. Chem. 18 (2008) 1949–1960.
[23] I.S. Maksymov, Optical switching and logic gates with hybrid plasmonic–photonic crystal nanobeam cavities, Phys. Lett. 375 (2011) 918–921.
[24] G.Y. Oh, D.G. Kim, Y.W. Choi, All-optical logic gate using waveguide-type SPR with Au/ZnO plasmon stack, Tech. Dig. 45 (2010) 374–375.
[25] J.H. Kim, B.K. Kang, Y.H. Park, Y.T. Byun, S. Lee, D.H. Woo, et al., All-optical AND gate using XPM wavelength converter, J. Opt. Soc. Korea 5 (2001) 25–28.
[26] S. Kaur, R.S. Kaler, Ultrahigh speed reconfigurable logic operations based on single semiconductor optical amplifier, J. Opt. Soc. Korea 16 (2012) 13–16.
[27] H. Wei, Z. Li, X. Tian, Z. Wang, F. Cong, N. Liu, S. Zhang, P. Nordlander, N.J. Halas, H. Xu, Quantum dot-based local field imaging reveals plasmon-based interferometric logic in silver nanowire networks, Nano Lett. 11 (2011) 471–475.
[28] A. Boltasseva, Plasmonic components fabrication via nanoimprint, J. Opt. A - Pure Appl. Opt. 11 (2009) 114001–114007.
[29] P.B. Johnson, R.W. Christy, Optical constants of the noble metals, Phys. Rev. B 6 (1972) 4370–4379.
[30] E. Pourali, M.A. Baboli, Design and analysis of an all optical OR gate using surface plasmon hopping along metallic nanorods, Phys. Scr. 90 (2015) 045501–045507.
[31] M. Akhlaghi, F. Emami, M.S. Sadeghi, M. Yazdanypoor, Simulation and optimization of nonperiodic plasmonic nano-particles, J. Opt. *Soc.* Korea 18 (2014) 82–88.
[32] J.M. Luck, Cantor spectra and scaling of gap widths in deterministic aperiodic systems, Phys. Rev. B 39 (1989) 5834–5849.
[33] A. Dolatabady, N. Granpayeh, All optical logic gates based on two dimensional plasmonic waveguides with nanodisk resonators, J. Opt. *Soc.* Korea 16 (2012) 432–442.
[34] P.P. Sahu, Theoretical investigation of all optical switch based on compact surface plasmonic two mode interference coupler, IEEE J. Light. *Technol.* 34 (2016) 1300–1305.
[35] N. Gogoi, P.P. Sahu, All optical switch using optically controlled two mode interference coupler, Appl. Opt. 51 (2012) 2601–2605.
[36] P.P. Sahu, All optical compact surface plasmonic two mode interference device for optical logic gates, Appl. Opt. 54 (2015) 1051–1057.